

Collapse simulations of a long span transmission tower-line system subjected to near-fault ground motions

Li Tian^{1a}, Haiyang Pan^{1b}, Ruisheng Ma^{1,2c} and Canxing Qiu^{*1}

¹School of Civil Engineering, Shandong University, Jinan, Shandong, 250061, China

²Centre for Infrastructure Monitoring and Protection, School of Civil and Mechanical Engineering, Curtin University, Kent Street, Bentley, WA 6102, Australia

(Received June 8, 2017, Revised August 22, 2017, Accepted September 5, 2017)

Abstract. Observations from past strong earthquakes revealed that near-fault ground motions could lead to the failure, or even collapse of electricity transmission towers which are vital components of an overhead electric power delivery system. For assessing the performance and robustness, a high-fidelity three-dimension finite element model of a long span transmission tower-line system is established with the consideration of geometric nonlinearity and material nonlinearity. In the numerical model, the Tian-Ma-Qu material model is utilized to capture the nonlinear behaviours of structural members, and the cumulative damage D is defined as an index to identify the failure of members. Consequently, incremental dynamic analyses (IDAs) are conducted to study the collapse fragility, damage positions, collapse margin ratio (CMR) and dynamic robustness of the transmission towers by using twenty near-fault ground motions selected from PEER. Based on the bending and shear deformation of structures, the collapse mechanism of electricity transmission towers subjected to Chi-Chi earthquake is investigated. This research can serve as a reference for the performance of large span transmission tower line system subjected to near-fault ground motions.

Keywords: long span transmission tower-line system; collapse simulation; near-fault ground motion; collapse fragility; collapse mechanism

1. Introduction

Transmission tower-line system consisting of electricity towers and transmission lines is categorized as a lifeline project in the seismic design community. Due to the dependency of other pivotal infrastructures on electricity, it is of significance to minimize the hazard of failure of transmission tower in earthquake and keep it functional after an earthquake event. However, statistics from past earthquakes revealed that electricity transmission towers were more vulnerable to earthquake excitations. For example, power supply was disrupted due to the damages of electricity transmission systems (such as collapsed towers, broken lines, et.al) in the 1994 Northridge earthquake and 1995 Kobe earthquake (Hall *et al.* 1996, Shinozuka 1995). Fig. 1 illustrates the failure of transmission tower in the Northridge earthquake. As shown in Fig. 2, the 1999 Chi-Chi earthquake (NCEE 1999) caused severe damage to electricity transmission systems, including 69 transmission lines destroyed, 15 towers collapsed and 26 towers tilted. In addition, Due to strong ground motions and secondary disasters, more than 20 towers collapsed in the 2008 Wenchuan earthquake (Zhang *et al.* 2008). These

failures of transmission towers are partially attributed to the near-fault ground motions. Compared with far-fault ground motions, near-fault ground motions are characterized by a large velocity pulse which means that structure will be exposed to the massive energy input in a short time. Excessive energy input may exceed the ultimate capacity of transmission tower, thus cause failures of members or even the collapse of structure. Therefore, it is of importance to investigate the collapse, failure mechanism and robustness of long span transmission tower-line system subjected to near-fault ground motions, and to improve the seismic capacity for these kinds of structure.

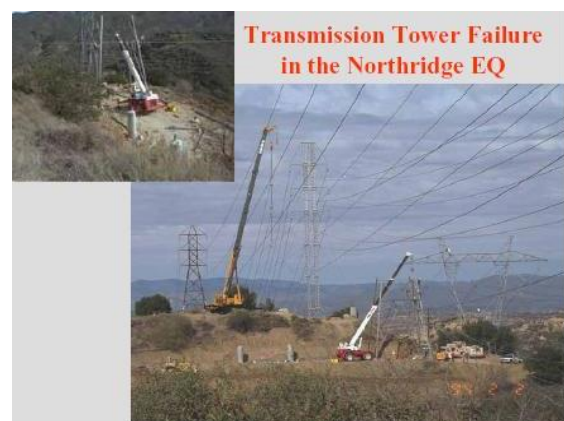


Fig. 1 The failure of transmission tower in the Northridge earthquake

*Corresponding author, Ph.D.

E-mail: qiucanxing@sdu.edu.cn.

^aAssociate Professor

^bM.D. Student

^cPH.D. Student



Fig. 2 The collapse of transmission tower in the Chi-Chi earthquake

There has been a significant amount of literatures dedicated to investigate seismic responses of transmission tower-line systems. Ghobarah *et al.* (1996) investigated the effect of multi-support excitations on the lateral seismic responses of overhead power transmission lines. Li *et al.* (2005, 2011) completed a series of investigation on dynamic responses of coupled transmission tower-line system subjected to seismic excitations, and proposed a simplified method to calculate its seismic response effectively. Tian *et al.* (2016a, 2016b, 2017a) studied the influence of spatial variation of seismic waves on the dynamic responses of transmission tower-line system based on experiments and numerical simulations, and investigated the progressive collapse of the structure subjected to extremely strong far-fault earthquake.

All these studies mentioned above are about the seismic responses of transmission tower-line system subjected to far-fault ground motions. Compared with far-fault ground motions, near-fault ground motions are more adverse and destructive, and have attracted wide attentions from researchers and engineers. Liao *et al.* (2001) compared the dynamic behaviors of reinforced concrete building subjected to near-fault and far-fault ground motions. The results indicated that long period responses in the response spectrum, PGV/PGA ratio and velocity pulse duration were higher than those from far-field ground motions. In addition, Liao *et al.* (2004) also investigated the dynamic responses of seismic isolated continuous girder bridges subjected to near-fault ground motions, in which the PGV/PGA value of near-fault earthquake records was defined as a key parameter governing the bridge response. Alavi and Krawinkler (2004) studied the responses characteristics of elastic and inelastic moment-resisting frame structures subjected to near-fault ground motions. The analysis demonstrated that near-fault ground motions had a different influence on longer-period structure and shorter-period structure. Kalkan and Kunnath (2006) investigated the consequences of well-known characteristics of near-fault ground motions on the seismic response of steel moment frames, which revealed that median maximum demands and the dispersion in the peak values were higher for near-fault records than far-fault motions. Phan *et al.* (2007) studied near-fault ground motion effects on reinforced concrete bridge columns subjected to near-fault ground motions and proposed a

framework for the evaluation of reinforced concrete bridge columns with respect to the control residual displacement. Li *et al.* (2017) evaluated the seismic responses of a super-span cable-stayed bridge subjected to near-fault ground motions, and the results showed that the near-fault pulse-type ground motions generated larger displacement and internal force to the bridge compared with the non-pulse ground motions. Wu *et al.* (2014) studied the seismic response of large crossing transmission tower-line system (LCTL) subjected to near-fault ground motions, and the results indicated that near-fault pulse-like ground motions imposed a larger seismic response to LCTL compared to far-fault ground motions. It was believed that the near-fault ground motion would have significant effect on the response of long span transmission tower-line system. These studies indicate that near-fault ground motions are quite different with 'ordinary' ground motions and impose large demands on structures (RC frame, bridges, *et al.*). From an importance point of view, dynamic responses and capacity of transmission tower-line system subjected to near-fault ground motions should be paid more attention. Up to date, very limited research has been completed to investigate the seismic responses of long span electricity transmission system subjected to near-fault ground motions. Therefore, it is necessary to investigate the ultimate capacity of long span transmission tower-line system subjected to near-fault ground motions.

Based on the above research status, the collapse analysis of a practical long span transmission tower-line system subjected to near-fault ground motion is conducted. A detailed 3D FE model of long span transmission tower-line system is established in ABAQUS according to engineering design. The Tian-Ma-Qu material model considering the damage cumulative effect is integrated into ABAQUS via a user subroutine to define material behavior VUMAT. The collapse simulation of the long span transmission tower-line system is performed using incremental dynamic analysis (IDA) method. The collapse fragility analysis and collapse mechanism of earthquake-induced are discussed in detail, respectively. As a result, this work will provide a reference for the seismic design of long span transmission tower-line system under near-fault seismic excitation.

2. Long span transmission tower-line system modeling

A long span transmission tower-line system across Yellow River (the sixth longest river in the world) in China is selected. The schematic diagram of the long span transmission tower-line system is shown in Fig. 3. The spans of the long span transmission tower-line system from north to south are 294, 1118 and 285 m, respectively. The system consists of four transmission towers and three span transmission lines. North and south side towers are tension-type, while north and south towers which are exactly the same are suspension-type.

A three-dimensional finite element model of the long span transmission tower-line system is established by using the commercial software ABAQUS in this study. The

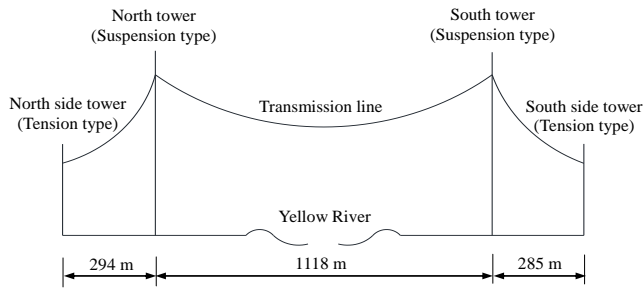


Fig. 3 Schematic diagram of long span transmission tower-line system



Fig. 4 Practical graph of suspension-type tower

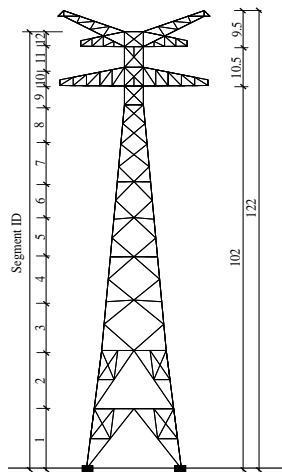


Fig. 5 Elevation of suspension-type tower (m)

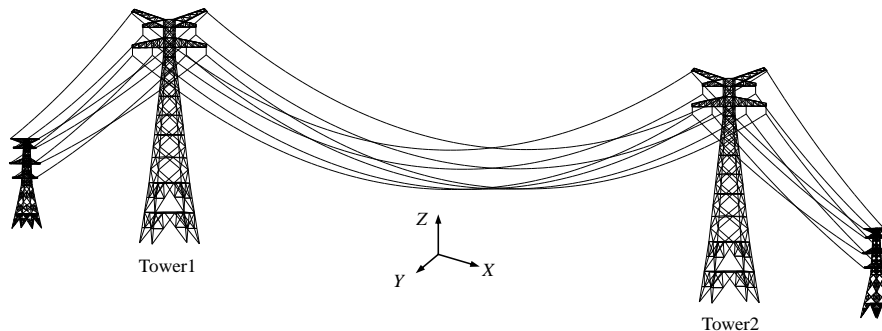


Fig. 6 Finite element model of long span transmission tower-line system

Table 1 Properties of conductor line and ground line

Type	Conductor line	Ground line
Designation	LHBGJ-400/95	OPGW-180
Total cross-section (mm ²)	501.02	175.2
Outside diameter (mm)	29.14	17.85
Elasticity modulus (GPa)	78000	170100
Coefficien of expansion (1/°C)	18.0E-6	12.0E-6
Mass per unit length (kg/km)	1856.7	1286

weight of the suspension-type tower is approximately 184 tons. Circular steel tubes of Q345 and Q235 are used as the main and diagonal members of the suspension-type tower, respectively. Fig. 4 shows practical graph of suspension-type tower. The elevation of suspension-type tower is shown in Fig. 5, in which the Segments 1 to 12 are illustrated along the height of the tower. The transmission towers including 1140 elements and 431 nodes are modeled by B31 beam elements. The supports of the transmission tower are assumed to be fixed. The first frequencies of the suspension-type tower in the longitudinal and transverse directions are 1.036 and 1.057 Hz, respectively.

There are 24 transmission lines including 6 ground lines and 18 conductor lines. The properties of conductor and ground lines are listed in Table 1. Both the transmission lines and insulators are modeled by truss element, and the elastic tension-only material property is assigned to the transmission lines that account for the geometric nonlinearity. The finite element model of the long span transmission tower-line system is illustrated in Fig. 6. The north and south suspension-type towers are denoted as Tower 1 and Tower 2 which are the main research objects in this study. The X, Y and Z directions of the model are expressed as the longitudinal, transverse and vertical direction of the long span transmission tower-line system, respectively.

3. Method for collapse simulation

Generally, the material constitutive model chosen for collapse analysis is an extremely crucial factor, which can affect the precise of numerical results directly. In this paper,

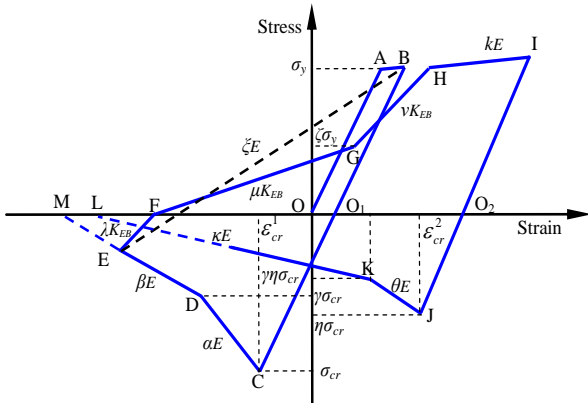


Fig. 7 Tian-Ma-Qu material model

the collapse of long span transmission tower-line system is simulated using Tian-Ma-Qu material model which has been verified and used in previous work (Tian *et al.* 2016c, Tian *et al.* 2017b). For concise consideration, the detailed mathematical expressions of Tian-Ma-Qu are not present here. Evidently, this model can capture the nonlinear behavior of the tube, including yielding, buckling, strain hardening, stiffness and strength degradations as shown in Fig. 7.

It is believed that the integral collapse of structure is caused by member failures and the buckling instability is the primary failure mode for steel components (steel tube, angle steel, *et al.*). However, it is inappropriate to delete a member directly when it buckles due to the existence of residual bearing capacity (Fig. 7). Therefore, the damage index D is introduced in this paper to identify the failure of member. This damage model consists of two parts (ultimate plastic damage and cumulative plastic damage), and has been calibrated in experiments (Dong and Shen 1996, Zhi *et al.* 2012). In this model, ‘0’ and ‘1’ denote undamaged state and fully damaged state of member, respectively. And at each time increment, the damage level of every member can be evaluated by the values of D which vary from 0 to 1.0. If the value of the D reaches 1.0, this member failed and its stiffness is degraded to zero.

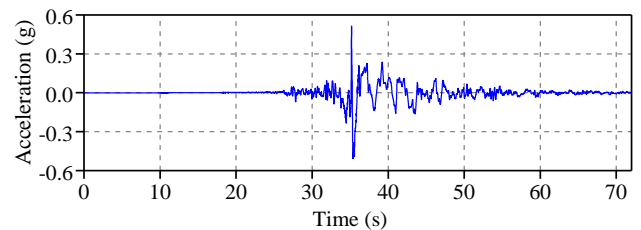
In this paper, the Tian-Ma-Qu material model, cumulative damage model and member failure criterion are introduced into the user material routine VUMAT to simulate the collapse of long span transmission tower subjected to near-fault ground motions. Generally, the collapse of structure is initiated by a local failure, and subsequently, partial or integral collapse of the structure will be triggered. According to the code for anti-collapse design of building structures (CECS 392-2014 2014), the tendency of horizontal displacement at the top of structure under the gravity can serve as an index to determine whether the structure is collapsed or not. If there is an increasing tendency of displacement time-histories, the structure can be regarded as collapsed.

4. Near-fault ground motions

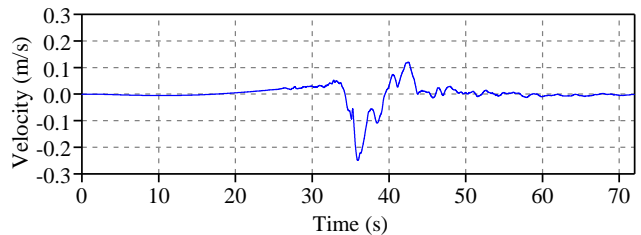
Ground motions close to a ruptured fault are

Table 2 Seismic wave records of near-fault ground motions

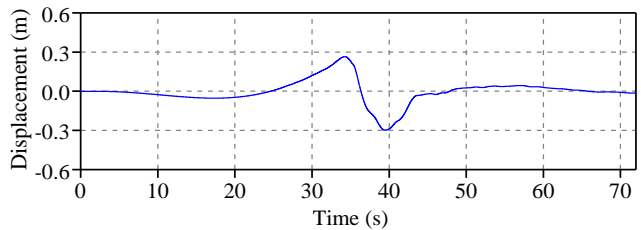
ID	Earthquake	Station	Distance/km	Magnitude/M
GM1	1999Chi-Chi	TCU049	3.76	7.6
GM2	1999Chi-Chi	TCU051	7.64	7.6
GM3	1999Chi-Chi	TCU052	0.66	7.6
GM4	1999Chi-Chi	TCU068	0.32	7.6
GM5	1999Chi-Chi	TCU075	0.89	7.6
GM6	1999Chi-Chi	TCU076	2.74	7.6
GM7	1999Chi-Chi	TCU082	5.16	7.6
GM8	1999Chi-Chi	TCU010 2	1.49	7.6
GM9	1994Northridge	LA Dam	5.92	6.7
GM10	1994Northridge	LSVH	8.44	6.7
GM11	1994Northridge	NFS	5.92	6.7
GM12	1994Northridge	NWH	5.48	6.7
GM13	1994Northridge	PKC	7.26	6.7
GM14	1994Northridge	RRS	6.5	6.7
GM15	1994Northridge	SCS	5.35	6.7
GM16	1994Northridge	SCS(E)	5.19	6.7
GM17	1994Northridge	SOVM	5.3	6.7
GM18	1980Irpinia Italy-01	STN	10.84	6.9
GM19	1999Kocaeli Turkey	Izmit	7.21	7.5
GM20	1999Duzce Turkey	Duzce	6.58	7.1



(a) Acceleration time history curve



(b) Velocity time history curve



(c) Displacement time history curve

Fig. 8 Time-history curves of typical near-fault seismic wave

significantly different from those observed further away from the seismic source. Near-fault ground motion, which has a large velocity pulse, may cause a large permanent displacement. In recent years, a lot of near-fault ground motion records are obtained by the strong earthquakes in the world. The near-fault ground motions which are summed to be restricted to within a distance of about 20 km from the ruptured fault, are considered in this paper (Bray and Rodriguez-Marek 2004).

Table 2 lists selected 20 typical natural seismic records, which include 8 Chi-Chi seismic waves, 9 Northridge seismic waves and 3 seismic waves regulated in the Federal Emergency Management Agency (FEMA) (FEMA-P695 2009). All these seismic records are selected from the database of Pacific Earthquake Engineering Research Center (PEER, <http://peer.berkeley.edu/>). It can be found that the magnitudes of all seismic waves are arranged from 6.7 to 7.6 M, and the fault distance is less than 20 km. Three components of seismic wave are applied along the longitudinal, transverse and vertical directions of the transmission tower-line system simultaneously. Among two horizontal components of each seismic record, one with larger peak ground acceleration (PGA) will be input along the longitudinal direction of the coupled system. Fig. 8 shows the acceleration, velocity and displacement time-histories of 1999 Chi-Chi earthquake recorded at the TCU068 station. It is obvious that the record contains a large pulse within the time range from 35 to 38 s.

5. Structural collapse analysis and discussion

The collapse of the long span transmission tower-line system shown in Fig. 6 subjected to near-fault ground motion is simulated using explicit integral method. Damping ratios of 2% and 1% are assumed for the transmission towers and transmission lines respectively, and the damping effect is simulated with Rayleigh damping model. The collapse PGAs of the transmission tower under different seismic excitations are analyzed by using IDA method. The collapse fragility analysis and collapse mechanism of the long span transmission tower-line system are discussed, respectively.

5.1 Collapse fragility analysis

Seismic fragility is a noteworthy problem for structures, especially lifeline projects, subjected to near-fault ground motions. The seismic fragility of structures can be evaluated by using fragility curves, which can be obtained from many kinds of seismic fragility analysis (FEMA-P695 2009, Rota *et al.* 2010, Billah *et al.* 2012, Lupoi *et al.* 2006). Fragility curves actually are the relationships between collapsed PGA and collapse probability of structure, and commonly obtained by IDA. The seismic fragility of long span transmission tower-line system is evaluated by IDA in this paper, and the detailed calculating processes are shown as below:

(1) The collapse analyses of long span transmission tower-line system subjected to near-fault ground motions

are conducted. Note that the maximum acceleration of horizontal seismic component along the longitudinal direction of the system is adjusted to 0.2g which is the design acceleration regulated in code (GB 50260-2013 2013), and the acceleration amplitudes of other two seismic components are adjusted in the equal proportion.

(2) The PGA along the longitudinal direction of the system is amplified gradually with the increment of 0.01 g, and an identical scale factor is applied to multi-components of ground motion. The curves of maximum displacements of the top of the tower are calculated using IDA method. Repeating the above analysis, the collapse PGAs of the tower under 20 near-fault ground motions are obtained.

(3) The collapse PGAs data in step 2 are fitted by the lognormal distribution (Inaudi and Makris 1996), and the fragility curve is obtained.

The collapse PGAs and damage positions of the long span transmission tower-line system under different near-fault ground motions are summarized in Fig. 9. It can be seen that the damage positions vary under different seismic excitations. The damage positions are mainly ranged from Segment 2 to 5, and these damage positions will lead to the collapse of the entire tower. It is evident that Segment 3 is the vulnerable region, and the damage probability of Segment 3, 5, 2 and 4 are 70, 20, 5 and 5% of all the potential collapse regions respectively, which indicates that Segment 3 has a higher possibility to become the initial collapse region than the other regions. Segment 3 should be treated as the weakest position of the tower where should be paid more attention for the seismic design. Fig. 9 also indicates that the collapse PGAs vary from 0.5 to 0.8 g under 20 near-fault ground motions, which are 2.5 to 4 times as the designed PGA. The dynamic capacity curves of the transmission tower under seven typical seismic excitations are plotted in Fig. 10. The maximum displacement curves in the two horizontal and vertical directions present linear characteristic when the PGAs are smaller than collapse critical values. However, when the PGAs exceed collapse critical values, the maximum displacements of the two horizontal and vertical directions increase sharply which are far beyond normal working condition.

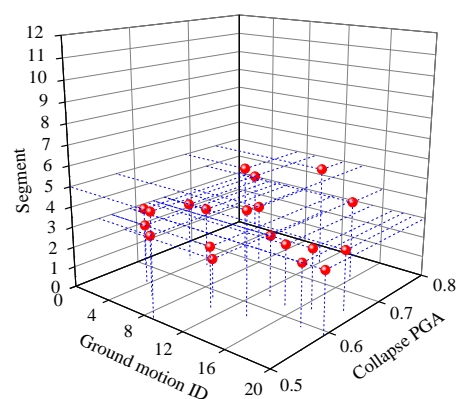


Fig. 9 Collapse PGAs and damage positions of transmission tower under different near-fault ground motions

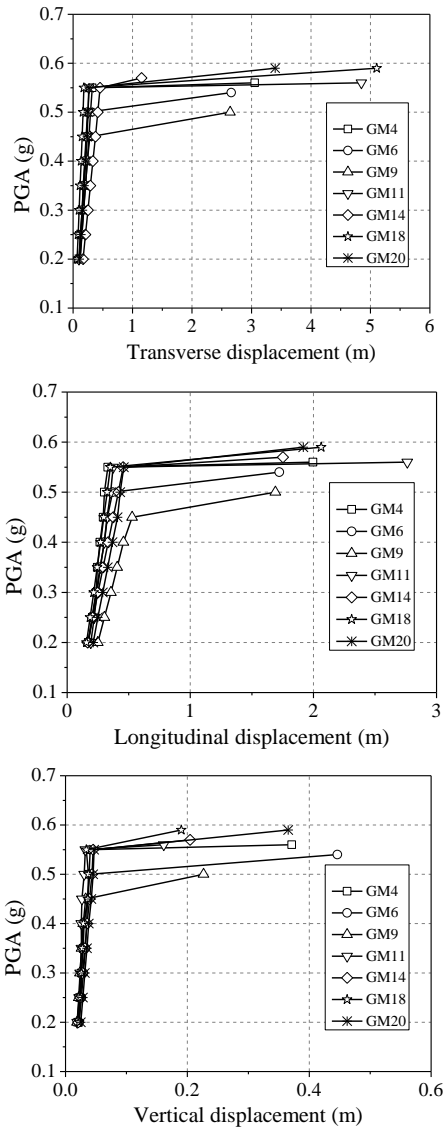


Fig. 10 The dynamic capacity curves of the transmission tower under different seismic excitations

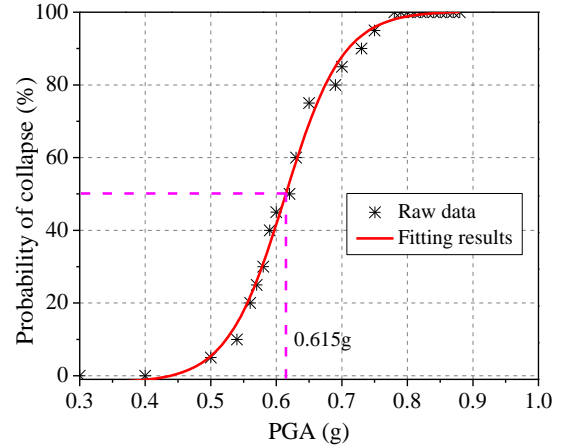


Fig. 11 Collapse fragility curve of the transmission tower under near-fault ground motions

The collapse fragility curve of the transmission tower under near-fault ground motions is plotted in Fig. 11. According to the seismic ground parameters zonation map of China (GB 18306-2015 2015), the PGA associated with the 2% probability of exceedance in 50 years (designated as rare ground motion) is 1.6 to 2.3 times that associated with the 10% probability of exceedance in 50 years (designated as basis ground motion). The PGA associated with the rare ground motion for the transmission tower changes from 0.32 to 0.46 g. It is suggested that the collapse probability under maximum considered earthquake (MCE) ground motions should be limited to 10% according to FEMA (FEMA-P695 2009). The collapse probability of the transmission tower under MCE ground motions is zero, which satisfies the collapse probability limit. However, the PGA associated with the 10^{-4} probability of exceedance in one year (designated as very rare ground motion) is 2.7 to 3.2 times that associated with the basis ground motion. The PGA associated with the very rare ground motion varies from 0.54 to 0.64 g. Considering the possibility of very rare

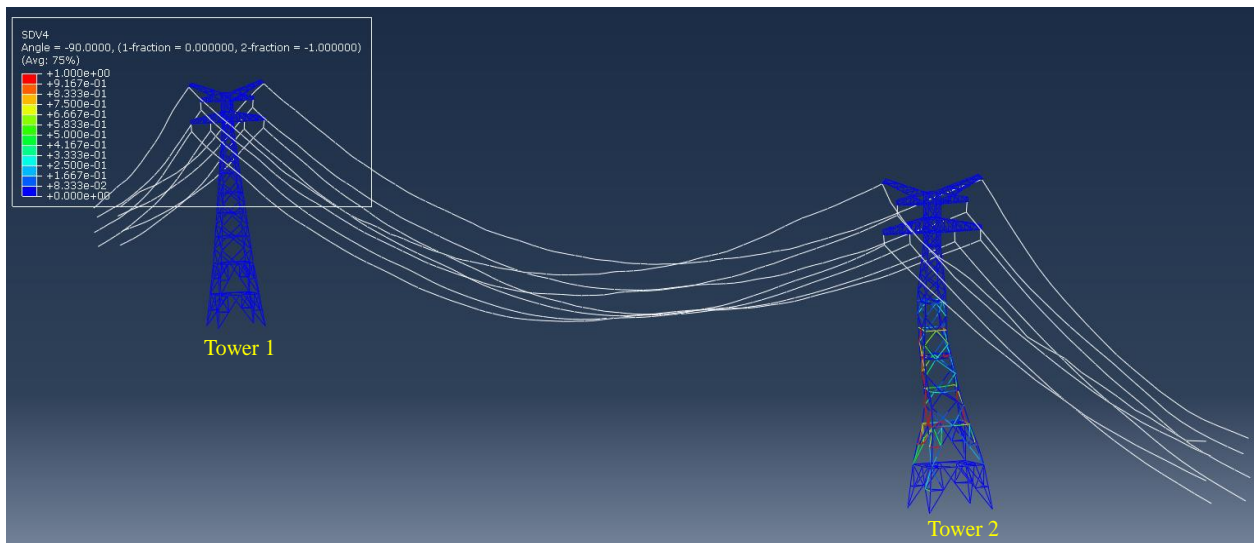


Fig. 12 Typical collapse mode of the transmission tower under the Chi-Chi earthquake ground motion (PGA= 0.54 g)

ground motion, the collapse probability of the transmission tower under MCE ground motions ranges from 5 to 60%, which shows that the collapse resistance should be improved.

To evaluate the structural collapse resistance capacity, the collapse margin ratio (CMR) is proposed in FEMA (FEMA 2009), which is defined by the following equation

$$CMR = IM_H / IM_{MCE} \quad (1)$$

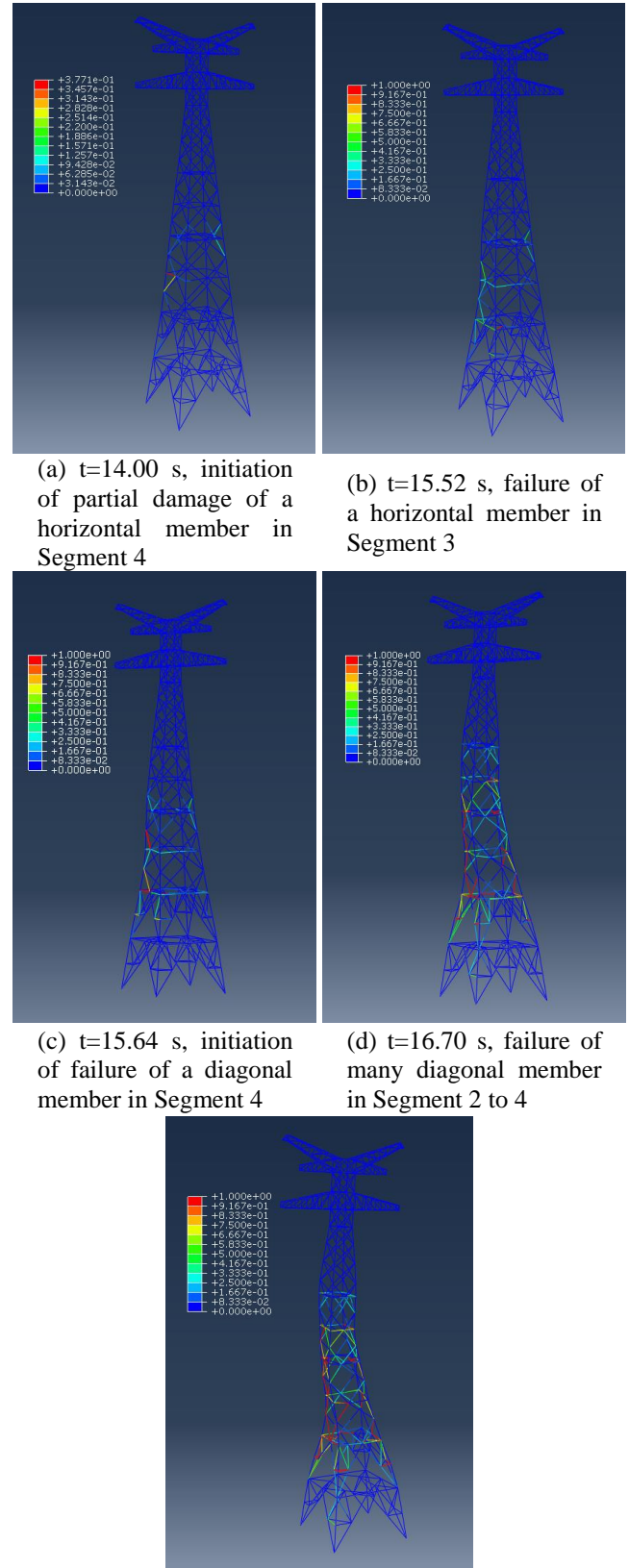
where, IM_H is the ground motion intensity subject to which the collapse possibility is 50%; IM_{MCE} is ground motion intensity corresponding to the design MCE level. As shown in Fig. 11, the PGA corresponding to the collapse possibility of 50% is 0.615g and the collapse margin ratio is ranged from 1.34 to 1.92 according to Eq. (1). It can be seen that the CMR is relatively small, which shows the long span transmission tower-line system is prone to collapse.

5.2 Collapse mechanism analysis

Chi-Chi earthquake (GM6) is selected as a typical input to investigate the collapse mechanism of the long span transmission tower-line system subjected to near-fault ground motions. The collapse mechanism and collapse process of the tower are discussed, respectively. To better reveal the collapse mechanism, the distributions of bending deformation and shear deformation of the tower along height are investigated and compared.

Fig. 12 illustrates the typical collapse mode of the transmission tower subjected to the Chi-Chi earthquake ground motion, in which the failed elements ($D=1.0$) are distributed in Segment2 to 5 of Tower 2, and it is consistent with the damage position in Fig. 9. It can be seen that the deformation of the Tower 2 is extremely large and exceeds the normal working limit, which leads to the collapse of the tower.

The collapse details of Tower 2 under the Chi-Chi earthquake excitations are shown in Fig. 13. At the initial stage, when $t=14.00$ s (Fig. 13(a)), the damage index D of the horizontal member 806 is equal to 0.3771 in Segment 4, which demonstrates that the member 806 has been damaged to some extent. When $t=15.52$ s (Fig. 13(b)), the damage index of the horizontal member 202 in Segment 3 reaches 1.0, and the member 202 loses bearing capacity. When $t=15.64$ s (Fig. 13(c)), the diagonal member 802 in Segment 4 begins to fail. The strain and force time history curves of the diagonal member 802 are plotted in Fig. 14. It can be found that the strain of the member 802 increases rapidly, which indicates the deformation is very large and the member has been destroyed. The internal force time history of the member 802 increases first and then decreases to zero, and this is because that the instability failure of the member occurs at first and then the member cannot bear the load anymore, which leads to the redistribution of the internal force of the tower. Subsequently, when $t=16.70$ s (Fig. 13(d)), many diagonal members fail in Segments 2 to 4, and the internal forces are redistributed to other structural members. The horizontal loads increase gradually and reach their load-carrying capacities. Finally, when $t=17.00$ s (Fig.



(a) $t=14.00$ s, initiation of partial damage of a horizontal member in Segment 4

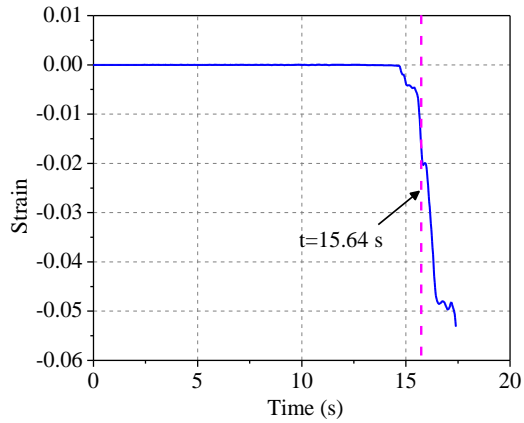
(b) $t=15.52$ s, failure of a horizontal member in Segment 3

(c) $t=15.64$ s, initiation of failure of a diagonal member in Segment 4

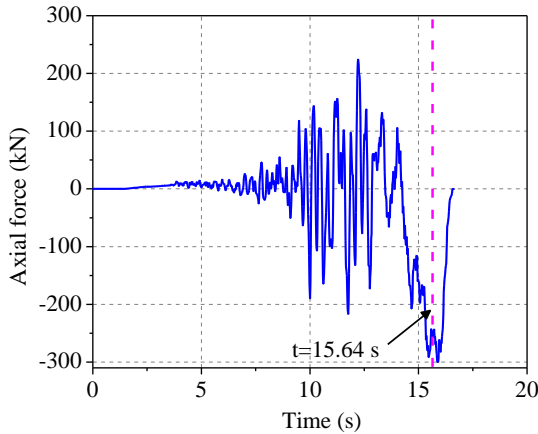
(d) $t=16.70$ s, failure of many diagonal members in Segment 2 to 4

(e) $t=17.00$ s, failure of many diagonal members in Segment 2 to 5

Fig. 13 Collapse details of Tower 2 under the Chi-Chi earthquake excitation



(a) Strain-time history curve



(b) Force-time history curve

Fig. 14 The strain-time and Force-time history curves of the failed member 321

13e), Segments 2 to 5 are severely damaged and most of connected members fail. The entire tower reaches its load-carrying capacity and starts to tilt. From the collapse process described above, the structural failure sequence proceeds as follows: from the horizontal member in Segment 3, to the diagonal member in Segment 4, and finally to many diagonal and horizontal members in Segments 2 to 5. It can be seen that the failure of diagonal and horizontal members will lead to the collapse of the tower.

The transverse, longitudinal and vertical displacement time histories at the top of Tower 2 subjected to the Chi-Chi ground motion are plotted in Fig. 15. When the tower starts to collapse, the displacements at the top of the tower increase rapidly. When $t=17.40$ s, the longitudinal, transverse and vertical displacements can reach 1.80, 2.69 and 0.45 m, respectively. It can be discovered that the displacements in three directions are greater than the allowable value of normal work. Fig. 15 indicates that the horizontal displacements are larger than the vertical displacement at the stage of collapse.

Transmission tower is one kind of space steel structure. The failure of main, diagonal and horizontal members may be caused by excessive bending and shear deformations, respectively. Bending deformation and shear deformation can be calculated as follows

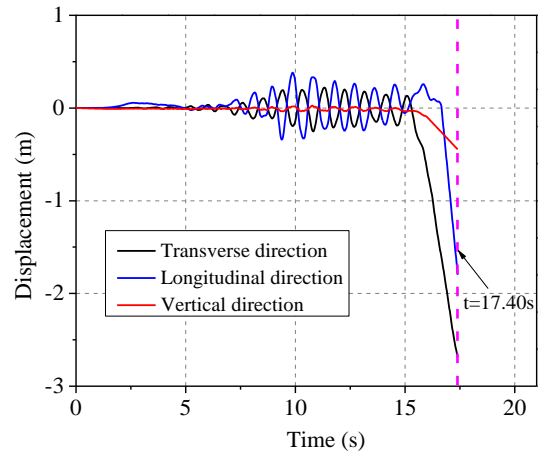
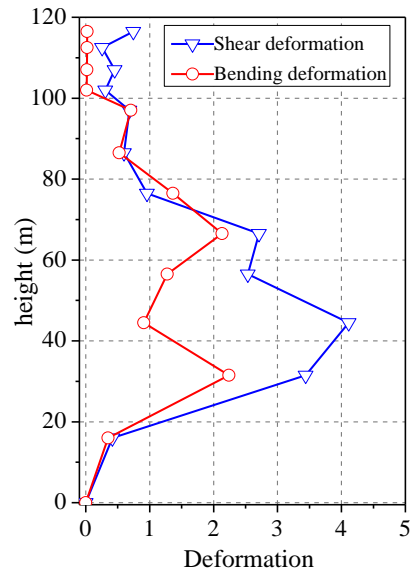
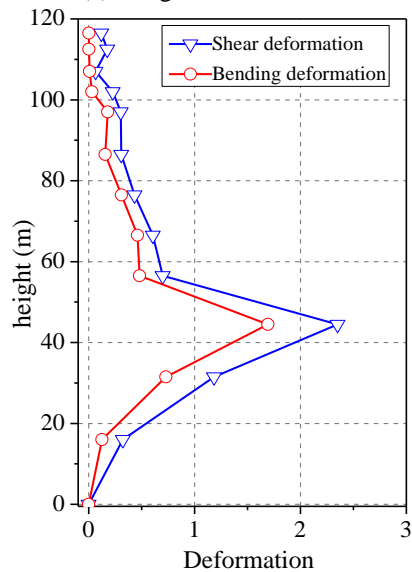


Fig. 15 The horizontal and vertical displacement time histories of Tower 2 under the Chi-Chi earthquake excitation



(a) Longitudinal direction



(b) Transverse direction

Fig. 16 Deformation distributions of the transmission tower along structural height

$$D_M = \max \left[(h_i - h_{i-1}) * (\theta_i(t) - \theta_{i-1}(t)) \right] \quad (2)$$

$$D_V = \max \left[u_i(t) - u_{i-1}(t) - \theta_i(t) * (h_i - h_{i-1}) \right] \quad (3)$$

where, i is the segment number; t is the time; $u_i(t)$ and $u_{i-1}(t)$ are the horizontal displacement time histories at the top and bottom of the segment i ; h_i and h_{i-1} are the height at the top and bottom of the segment i ; $\theta_i(t)$ and $\theta_{i-1}(t)$ are the torsional displacement time histories at the top and bottom of the segment i .

The deformation distributions of the tower along structural height are plotted in Fig. 16, in which the deformations of Segment 2 to 5 in the longitudinal direction and Segment 3 in the transverse direction change sharply, and these are consistent with the weak position of the tower. Fig. 16 indicates that the shear deformations of the tower in longitudinal and transverse directions are larger than those of the bending deformations, which can lead to the failure of diagonal and horizontal members, and these results agree with the failure member shown in Fig. 13. Based on the above analysis, it can be obtained that the failure of diagonal and horizontal members are caused by excessive shear deformation, while excessive bending deformation results in the failure of main member. Therefore, the reasons for the failure of transmission tower can be determined by the bending and shear deformations.

6. Conclusions

In this paper, the collapse analysis of a long span transmission tower-line system under near-fault ground motions is carried out. With consideration of cumulative damage effect, buckling effect and failure criterion, Tian-Ma-Qu material model is utilized to capture the nonlinear behavior of members in structure. Seismic fragility and collapse mechanism of long span transmission tower-line system subjected to near-fault ground motions are discussed. Based on the result database obtained from this investigation, the following significant conclusions are drawn:

- The Tian-Ma-Qu material model is effective to capture the nonlinear behaviors of member, simulate the realistic collapse process of long span transmission tower-line system, and evaluate the seismic robustness of structure subjected to near-fault ground motions.
- The damage probability of Segment 3 is 70% of all the potential collapsed regions, which means more attentions should be paid to seismic design of this structure. Due to the redistribution of internal force, the failure of a diagonal or horizontal member is able to cause continuous failures of members, and results in the collapse of whole structure eventually.
- Notwithstanding the transmission tower could satisfy the collapse resistant requirements under rare ground motion, the collapse resistant capacity of the tower should be noticed and improved. Results from CMR analysis show that long span transmission tower is

prone to collapse when it subjects to near-fault ground motions.

- Excessive shear deformation leads to the failure of diagonal and horizontal members, and excessive bending deformation results in the failure of main member. Failure modes of members can be obtained from the distributions of the bending and shear deformations along height of transmission tower.

Acknowledgements

This research was financially supported by the National Natural Science Foundation of China under Awards No. 51578325 and 51778347.

References

- Alavi, B. and Krawinkler, H. (2004), "Behavior of moment-resisting frame structures subjected to near-fault ground motions", *Earthq. Eng. Struct. D.*, **33**(6), 687-706.
- Billah, A.M., Alam, M.S. and Bhuiyan, M.R. (2012), "Fragility analysis of retrofitted multicolumn bridge bent subjected to near-fault and far-field ground motion", *J. Bridge. Eng.*, **18**(10), 992-1004.
- Bray, J.D. and Rodriguez-Marek, A. (2004), "Characterization of forward-directivity ground motions in the near-fault region", *Soil Dyn. Earthq. Eng.*, **24**(11), 815-828.
- CECS 392-2014 (2014), Code for anti-collapse design of building structures, China Planning Press; Beijing, China. (in Chinese)
- GB 50260-2013 (2013), Code for seismic design of electrical installations, China Architecture & Building Press; Beijing, China. (in Chinese)
- GB 18306-2015 (2015), Seismic ground motion parameters zonation map of china, Standardization Administration of China Press; Beijing, China. (in Chinese)
- Dong, B. and Shen, Z.Y. (1996), "Analysis of damage accumulation for steel tower structure subjected to earthquake", *Spec. Struct.*, **13**(3), 30-32. (in Chinese)
- FEMA-P695 (2009), "Quantification of building seismic performance factors", Washington, DC, USA.
- Ghobarah, A., Aziz, T.S. and El-Attar, M. (1996), "Response of transmission lines to multiple support excitation", *Eng. Struct.*, **18**(12), 936-946.
- Hall, J.F., Holmes, W.T. and Somers, P. (1996), "Northridge earthquake of January 17, 1994", Earthquake Engineering Research Institute, California, USA.
- Inaudi, J.A. and Makris, N. (1996), "Time-domain analysis of linear hysteretic damping", *Earthq. Eng. Struct. D.*, **25**(6), 529-546.
- Kalkan, E. and Kunnath, S.K. (2006), "Effects of fling step and forward directivity on seismic response of buildings", *Earthq. spectra*, **22**(2), 367-390.
- Li, H.N., Shi, W.L., Wang, G.X. and Jia, L.G. (2005), "Simplified models and experimental verification for coupled transmission tower-line system to seismic excitations", *J. Sound. Vib.*, **286**(3), 565-585.
- Li, H.N., Bai, F.L., Tian, L. and Hao, H. (2011), "Response of a transmission tower-line system at a canyon site to spatially varying ground motions", *J. Zhejiang Univ. - SC. A*, **12**(2), 103-120.
- Li, S., Zhang, F. and Wang, J.Q. (2017), "Effects of near-fault motions and artificial pulse-type ground motions on super-span

- cable-stayed bridge systems”, *J. Bridge. Eng.*, **22**(3).
- Liao, W.I., Loh, C.H. and Wan, S. (2001), “Earthquake responses of RC moment frames subjected to near-fault ground motions”, *Struct. Des. Tall Spec. Build.*, **10**(3), 219-229.
- Liao, W.I., Loh, C.H. and Lee, B.H. (2004), “Comparison of dynamic response of isolated and non-isolated continuous girder bridges subjected to near-fault ground motions”, *Eng. Struct.*, **26**(14), 2173-2183.
- Lupoi, G., Franchin, P., Lupoi, A. and Pinto, P.E. (2006), “Seismic fragility analysis of structural systems”, *J. Eng. Mech.*, **132**(4), 385-395.
- NCREE (1999), “Investigation Report of Chi-Chi Earthquake”, National Center for Research on Earthquake Engineering, Taiwan.
- Phan, V., Saiidi, M.S. and Anderson, J. (2007), “Near-fault ground motion effects on reinforced concrete bridge columns”, *J. Eng. Mech.*, **133**(7), 982-989.
- Rota, M., Penna, A. and Magenes, G. (2010), “A methodology for deriving analytical fragility curves for masonry buildings based on stochastic nonlinear analyses”, *Eng. Struct.*, **32**(5), 1312-1323.
- Shinozuka, M. (1995), “The Hanshin-Awaji earthquake of January 17, 1995 Performance of life lines”, Report NCEER-95-0015, NCEER.
- Tian, L., Gai, X., Qu, B., Li, H.N. and Zhang, P. (2016a), “Influence of spatial variation of ground motions on dynamic responses of supporting towers of overhead electricity transmission systems: an experimental study”, *Eng. Struct.*, **128**, 67-81.
- Tian, L., Ma, R.S., Li, H.N. and Wang, Y. (2016b), “Progressive collapse simulation of power transmission tower-Line system under extremely strong earthquake”, *J. Struct. Stab. D.*, **16**(1), 1-21.
- Tian, L., Ma, R.S. and Qu, B. (2016c), “Development of a nonlinear material model for steel members under cyclic axial loading”, Technical Report No. 2016-2, Shandong University, Jinan, China.
- Tian, L., Gai, X. and Qu, B. (2017a), “Shake table tests of steel towers supporting extremely long-span electricity transmission lines under spatially correlated ground motions”, *Eng. Struct.*, **132**, 791-807.
- Tian, L., Ma, R.S., Pan, H.Y., Qiu, C.X. and Li, W.F. (2017b), “Progressive collapse analysis of long-span transmission tower-line system under multi-component seismic excitations”, *Adv. Struct. Eng.*, 1-13.
- Wu, G., Zhai, C.H., Li, S. and Xie, L.L. (2014), “Effects of near-fault ground motions and equivalent pulses on Large Crossing Transmission Tower-line System”, *Eng. Struct.*, **77**, 161-169.
- Zhang, Z.Y., Zhao, B. and Cao, W.W. (2008), “Investigation and preliminary analysis of damages on the power grid in the Wenchuan Earthquake of M8.0”, *Electric Pow. Technol. Economics*, **20**(4), 1-4. (in Chinese)
- Zhi, X.D., Nie, G.B., Fan, F. and Shen, S.Z. (2012), “Vulnerability and risk assessment of single-layer reticulated domes subjected to earthquakes”, *J. Struct. Eng.*, **138**(12), 1505-1514.